

Inclusion of 2,4- and 2,5-Diphenyloxazole by γ -Cyclodextrin in Aqueous Solution

Sanyo Hamai

Department of Chemistry, Faculty of Education and Human Studies, Akita University,
1-1 Tegata Gakuen-machi, Akita 010-8502

Received November 26, 2007; E-mail: hamai@ipc.akita-u.ac.jp

In aqueous solution, the interactions of 2,4- and 2,5-diphenyloxazole (2,4- and 2,5-DPO) with β - and γ -cyclodextrin (β - and γ -CD) have been examined by means of absorption and fluorescence spectroscopies. γ -CD forms a 2:1 host–guest inclusion complex with 2,4-DPO, whereas β -CD forms a 1:1 inclusion complex with 2,4-DPO. Equilibrium constants for the formation of these inclusion complexes have been evaluated. Upon the addition of alcohol to 2,4-DPO solution containing γ -CD, the 2:1 γ -CD–2,4-DPO inclusion complex accommodates alcohol to form a 2:2:1 γ -CD–alcohol–2,4-DPO inclusion complex. The equilibrium constant for the formation of the 2:2:1 inclusion complex increases as the alkyl chain of the alcohol is lengthened from 1-pentanol to 1-heptanol. A similar trend in the magnitude of the equilibrium constant has been observed for diols (1,9-nonanediol and 1,10-decanediol). In contrast to 2,4-DPO, 2,5-DPO forms a 1:1 γ -CD–2,5-DPO inclusion complex at a low concentration of 2,5-DPO. At a high concentration of 2,5-DPO, excimer fluorescence of 2,5-DPO has been observed in the presence of γ -CD. From simulations of excimer fluorescence intensity as a function of γ -CD concentration, the excimer fluorescence is ascribed to both a 1:2 γ -CD–2,5-DPO inclusion complex and a 2:2 γ -CD–2,5-DPO inclusion complex.

Cyclodextrins (CDs), which are cyclic oligosaccharides, have more than five D-glucopyranose residues.¹ There is a hydrophobic cavity in the molecular center of CDs. An organic molecule of appropriate dimensions can be incorporated into the CD cavity to form a 1:1 host–guest inclusion complex. γ -CD, which is composed of eight D-glucopyranose residues, has a cavity wider than those of α - and β -CD, which are composed of six and seven D-glucopyranose residues, respectively. In some cases therefore, γ -CD forms a 1:2 host–guest inclusion complex besides a 1:1 inclusion complex; 1:2 γ -CD–guest inclusion complexes have been observed for Methyl Orange, Methylene Blue, Pyronine B, thionine, 2-dibenzofuranol, etc.^{2–6} In addition to 1:2 inclusion complexes, γ -CD forms 2:2 host–guest inclusion complexes,^{7–12} which are produced by association of the 1:1 inclusion complexes, although β -CD also forms a 2:2 inclusion complex.^{13–15}

The position of a substituent in a guest molecule affects the equilibrium constant for the formation of an inclusion complex with CD. Because of steric hindrance and/or different orientation in incorporating a guest molecule into a CD cavity, the equilibrium constants for positional isomers are different from each other. For *o*-, *m*-, and *p*-chlorocinnamic acid and *o*-, *m*-, and *p*-methoxycinnamic acid, the equilibrium constants of β -CD are 761, 1110, 595, 61, 451, and 658 mol^{−1} dm³, respectively.¹⁶ For 3- and 4-methylphenylacetate, the equilibrium constants of β -CD are 11.9 ± 1.4 and 40.4 ± 1.7 mol^{−1} dm³, respectively.¹⁷ In the case of 3- and 4-methoxyphenylacetate, the equilibrium constants of β -CD are 38.0 ± 1.1 and 69.3 ± 1.6 mol^{−1} dm³, respectively.¹⁷

In heterocyclic compounds, there may be isomers due to the different position of the heteroatom(s). In the case of benzoquinolines, the position of a nitrogen atom in the three fused

benzene rings likely affects the interactions with CDs. Recently, we have investigated the inclusion behavior of three benzoquinoline isomers by CDs.¹⁸ γ -CD forms 1:1 inclusion complexes with benzo[*f*]quinoline and phenanthridine, while a benzo[*h*]quinoline solution becomes turbid in the presence of γ -CD. Excimer fluorescence has been observed only for the 2:2 γ -CD–benzo[*f*]quinoline inclusion complex, which is formed by the association of 1:1 γ -CD–benzo[*f*]quinoline inclusion complexes. In addition to the difference in magnitude of the equilibrium constant for the formation of the 1:1 inclusion complex, the 1:1 inclusion complexes of benzo[*f*]quinoline and phenanthridine behave differently towards their association.

2,5-Diphenyloxazole (2,5-DPO) is a fluorescent compound, which is often used for scintillation counting. Agbaria and Gill have reported that 2,5-DPO emits excimer fluorescence in the presence of γ -CD.^{19,20} They have suggested that a 1:2 γ -CD–2,5-DPO inclusion complex is formed, and that the 1:2 inclusion complexes aggregate to form extended linear beads. Excimer fluorescence has been ascribed to the 1:2 γ -CD–2,5-DPO inclusion complex and its aggregate in γ -CD solution.^{19,20}

2,4-Diphenyloxazole (2,4-DPO) is a positional isomer of 2,5-DPO. Two phenyl groups in 2,5-DPO are located on both sides of an oxygen atom in an oxazole ring, respectively, whereas two phenyl groups in 2,4-DPO are located on both side of a nitrogen atom in an oxazole ring, respectively (Chart 1). Consequently, the two DPO molecules are nearly the same molecular shape, differing in the position of an oxygen atom and a nitrogen atom or interchanging the positions of these hetero-atoms.

To our knowledge, there have been no studies in which the complexation of CD with 2,4-DPO has been examined. We

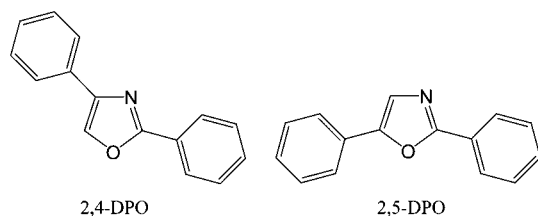


Chart 1.

have been interested in the interactions of γ -CD with the two DPO isomers, because it has been suggested that a single γ -CD molecule can accommodate two 2,5-DPO molecules. Thus, we have examined the inclusion modes of γ -CD towards 2,4-DPO. Two γ -CD molecules have been found to accommodate a single 2,4-DPO molecule. To compare the interactions between γ -CD and DPOs, we have also examined the complexation of γ -CD and 2,5-DPO through the excimer fluorescence of 2,5-DPO. We have further investigated the effects of alcohols on the formation of the inclusion complex of γ -CD with 2,4-DPO.

Experimental

γ -Cyclodextrin (γ -CD), which was purchased from Wako Pure Chemical Industries, Ltd., was used as received. β -Cyclodextrin (β -CD), which was purchased from Nacalai Tesque, Inc., was twice recrystallized from water. 2,4-Diphenyloxazole (2,4-DPO) and 2,5-diphenyloxazole (2,5-DPO), which were obtained from Tokyo Chemical Industry Co., Ltd., were used as received. 1-Pentanol and 1-hexanol, purchased from Wako Pure Chemical Industries, Ltd., were used without further purification. 1-Heptanol, 1,9-nonanediol, 1,10-decanediol, and 1,12-dodecanediol, obtained from Tokyo Chemical Industry Co., Ltd., were used as received. Aqueous solutions of 2,4-DPO and 2,5-DPO, which were used for the preparation of sample solutions, were prepared by submerging their crystals in water for a few days in the dark. The concentrations of 2,4- and 2,5-DPO were estimated under the assumption that their molar absorption coefficients in water are the same as those in methanol.

Absorption spectra were recorded on a Shimadzu UV-2450 spectrophotometer. Fluorescence spectra were taken with a Shimadzu RF-501 spectrofluorometer equipped with a cooled Hamamatsu R-943 photomultiplier. The fluorescence spectra were corrected for the spectral response of the fluorometer. Spectroscopic measurements were made at $25 \pm 0.1^\circ\text{C}$.

Results and Discussion

Inclusion of 2,4-DPO by γ -CD. Figure 1 shows absorption spectra of 2,4-DPO ($2.8 \times 10^{-6} \text{ mol dm}^{-3}$) in aqueous solutions containing several concentrations of γ -CD. Upon the addition of γ -CD, the absorbance of 2,4-DPO in aqueous solution is slightly increased over the wavelength range examined, suggesting interaction of γ -CD with 2,4-DPO.

Figure 2 depicts fluorescence spectra of 2,4-DPO ($2.8 \times 10^{-6} \text{ mol dm}^{-3}$) in aqueous solutions containing various concentrations of γ -CD. When γ -CD is added to 2,4-DPO solution, the 2,4-DPO fluorescence is reduced in intensity. At the same time, the intensity of a shoulder at about 370 nm surpasses the intensity of a peak at 390 nm, the fluorescence band being maximized at 365 nm at a γ -CD concentration of $1.0 \times 10^{-2} \text{ mol dm}^{-3}$, because the fluorescence maximum at

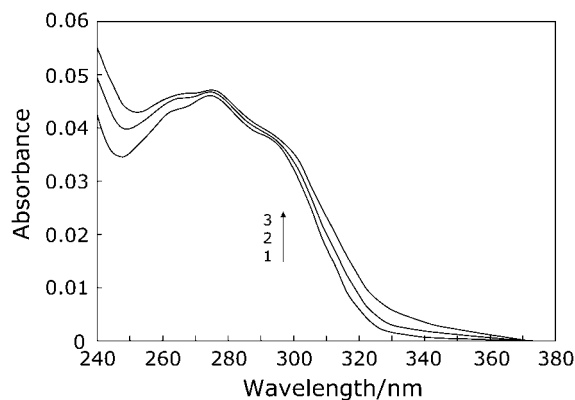


Figure 1. Absorption spectra of 2,4-DPO ($2.8 \times 10^{-6} \text{ mol dm}^{-3}$) in aqueous solutions containing several concentrations of γ -CD. Concentration of γ -CD: (1) 0, (2) 3.0×10^{-3} , and (3) $1.0 \times 10^{-2} \text{ mol dm}^{-3}$.

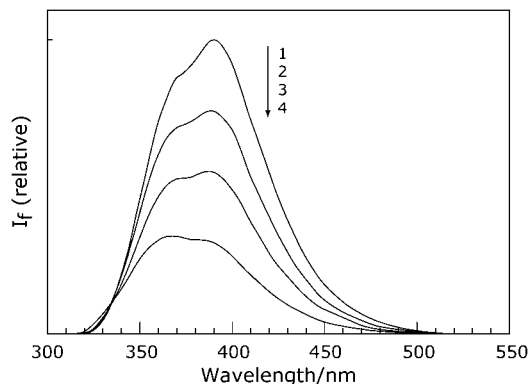


Figure 2. Fluorescence spectra of 2,4-DPO ($2.8 \times 10^{-6} \text{ mol dm}^{-3}$) in aqueous solutions containing various concentrations of γ -CD. Concentration of γ -CD: (1) 0, (2) 3.0×10^{-3} , (3) 5.0×10^{-3} , and (4) $1.0 \times 10^{-2} \text{ mol dm}^{-3}$. $\lambda_{\text{ex}} = 295 \text{ nm}$.

390 nm in the absence of γ -CD is significantly decreased in intensity compared to the shoulder at about 370 nm.

When γ -CD forms a 1:1 inclusion complex with 2,4-DPO, the equation (double reciprocal plot) holds for the fluorescence intensity:

$$1/(I_f - I_f^0) = 1/a + 1/(aK[\gamma\text{-CD}]). \quad (1)$$

Here, I_f and I_f^0 are the fluorescence intensities in the presence and absence of γ -CD, respectively, and a , K , and $[\gamma\text{-CD}]$ are instrumental constants including the fluorescence quantum yields of free 2,4-DPO and the 1:1 inclusion complex, the equilibrium constant for the formation of the 1:1 γ -CD–2,4-DPO inclusion complex, and the γ -CD concentration, respectively. Figure 3a exhibits a double reciprocal plot for the fluorescence intensity of 2,4-DPO ($2.8 \times 10^{-6} \text{ mol dm}^{-3}$) in aqueous solution containing γ -CD. The plot does not show a straight line, indicating that the γ -CD–2,4-DPO inclusion complex does not have a 1:1 stoichiometry concerning γ -CD and 2,4-DPO. There may be a possibility that a 2:1 γ -CD–2,4-DPO inclusion complex ($(\gamma\text{-CD})_2 \cdot 2,4\text{-DPO}$) is formed, because 2,4-DPO is long in molecular shape.

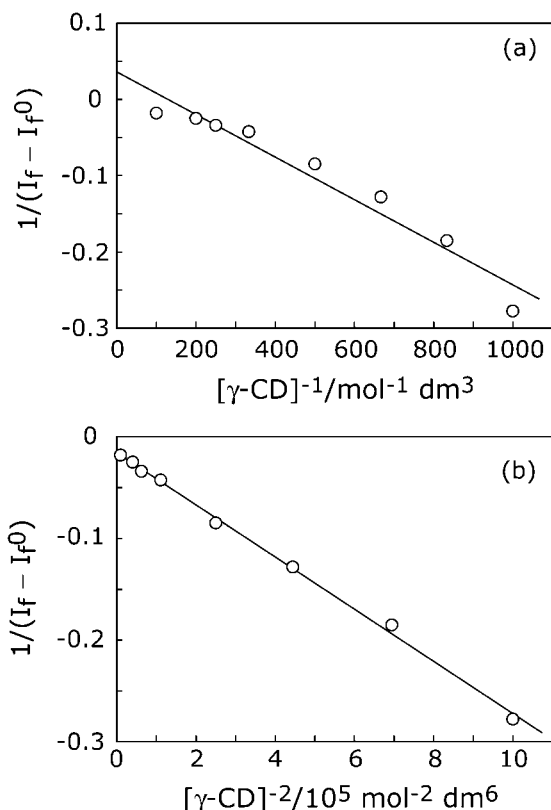


Figure 3. (a) Plot of $1/(I_f - I_f^0)$ against $1/[\gamma\text{-CD}]$ for 2,4-DPO in aqueous solution containing $\gamma\text{-CD}$. (b) Plot of $1/(I_f - I_f^0)$ against $1/[\gamma\text{-CD}]^2$ for 2,4-DPO in aqueous solution containing $\gamma\text{-CD}$. $[2,4\text{-DPO}] = 2.8 \times 10^{-6} \text{ mol dm}^{-3}$. $\lambda_{\text{ex}} = 295 \text{ nm}$. $\lambda_{\text{obs}} = 380 \text{ nm}$.



Here, K_1 is the equilibrium constant for the formation of the 2:1 $\gamma\text{-CD}$ -2,4-DPO inclusion complex. In this case, a plot of $1/(I_f - I_f^0)$ against $1/[\gamma\text{-CD}]^2$ should exhibit a straight line.

$$1/(I_f - I_f^0) = 1/b + 1/(bK_1[\gamma\text{-CD}]^2), \quad (3)$$

where b and K_1 are instrumental constants including the fluorescence quantum yields of free 2,4-DPO and the 2:1 $\gamma\text{-CD}$ -2,4-DPO inclusion complex, and the equilibrium constant for the formation of the 2:1 $\gamma\text{-CD}$ -2,4-DPO inclusion complex, respectively. Figure 3b shows a plot based on eq 3, which exhibits a straight line, indicating that the 2:1 $\gamma\text{-CD}$ -2,4-DPO inclusion complex is produced. From the plot shown in Figure 3b, the K_1 value is evaluated to be $61000 \text{ mol}^{-2} \text{dm}^6$. Because $\gamma\text{-CD}$ has the widest cavity among α -, β -, and γ -CDs, two guest molecules are likely accommodated within the $\gamma\text{-CD}$ cavity rather than a single guest molecule being accommodated within two $\gamma\text{-CD}$ cavities. For 2,4-DPO, however, two $\gamma\text{-CD}$ molecules are bound to a single 2,4-DPO molecule, forming the 2:1 $\gamma\text{-CD}$ -2,4-DPO inclusion complex.

The 2:1 $\gamma\text{-CD}$ -2,4-DPO inclusion complex would be formed stepwise through the formation of the 1:1 $\gamma\text{-CD}$ -2,4-DPO inclusion complex. However, the data of the observed fluorescence intensity exhibit very good linearity for the plot

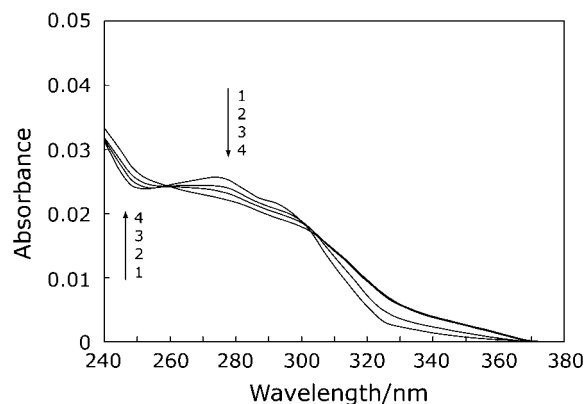


Figure 4. Absorption spectra of 2,4-DPO ($1.4 \times 10^{-6} \text{ mol dm}^{-3}$) in aqueous solutions containing $\gamma\text{-CD}$ ($3.0 \times 10^{-3} \text{ mol dm}^{-3}$) and various concentrations of PeOH. Concentration of PeOH: (1) 0, (2) 2.76×10^{-3} , (3) 9.20×10^{-3} , and (4) $2.76 \times 10^{-2} \text{ mol dm}^{-3}$.

of $1/(I_f - I_f^0)$ against $1/[\gamma\text{-CD}]^2$ as shown in Figure 3b. Consequently, the 2:1 $\gamma\text{-CD}$ -2,4-DPO inclusion complex is formed as if the formation proceeds in a single step, probably because the equilibrium constant of the formation of the 2:1 inclusion complex from the 1:1 $\gamma\text{-CD}$ -2,4-DPO inclusion complex and additional $\gamma\text{-CD}$ is very large.

We next examined the interactions of $\beta\text{-CD}$ with 2,4-DPO. The formation of a 1:1 inclusion complex of $\beta\text{-CD}$ with 2,4-DPO was confirmed from the linearity of a double reciprocal plot for the 2,4-DPO fluorescence intensity. The equilibrium constant (K) for the formation of the 1:1 $\beta\text{-CD}$ -2,4-DPO inclusion complex was estimated to be $760 \pm 100 \text{ mol}^{-1} \text{dm}^3$, which is close to the equilibrium constant ($685 \text{ mol}^{-1} \text{dm}^3$) of naphthalene.¹³ Although 2,4-DPO is almost a linear molecule, its shape is slightly bent. Consequently, an additional $\beta\text{-CD}$ molecule may not bind a 2,4-DPO molecule located within the $\beta\text{-CD}$ cavity, probably because there is steric hindrance from the $\beta\text{-CD}$ molecule bound to the 2,4-DPO molecule. Two $\gamma\text{-CD}$ molecules having a wide cavity, however, may accommodate a single 2,4-DPO, facing each other.

Effects of Alcohols on the Incorporation of 2,4-DPO into the $\gamma\text{-CD}$ Cavity. Harada et al. have reported that inclusion complexes are formed between poly(ethylene glycol) and not $\beta\text{-CD}$ but $\alpha\text{-CD}$.²¹ Poly(propylene glycol), which has methyl side chains, forms inclusion complexes with $\beta\text{-CD}$ and $\gamma\text{-CD}$, although $\alpha\text{-CD}$ does not form inclusion complexes with poly(ethylene glycol) of any molecular weight. In addition, it has been reported that 1,1'-diheptyl-4,4'-bipyridyl dibromide scarcely forms an inclusion complex with $\gamma\text{-CD}$, due to the $\gamma\text{-CD}$ cavity being too large to closely include a hydrophobic heptyl-chain of 1,1'-diheptyl-4,4'-bipyridyl dibromide.²² In this study, therefore, we have neglected the formation of an inclusion complex of $\gamma\text{-CD}$ with alcohol.

Figure 4 illustrates absorption spectra of 2,4-DPO ($1.4 \times 10^{-6} \text{ mol dm}^{-3}$) in aqueous solution containing $\gamma\text{-CD}$ ($3.0 \times 10^{-3} \text{ mol dm}^{-3}$) and various concentrations of 1-pentanol (PeOH). As the PeOH concentration is increased, the absorption peak at around 275 nm decreases, suggesting the formation of an inclusion complex of $\gamma\text{-CD}$ with PeOH and 2,4-DPO. Figure 5 exhibits fluorescence spectra of 2,4-DPO

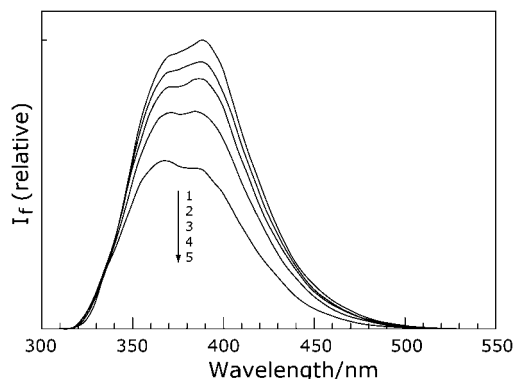


Figure 5. Fluorescence spectra of 2,4-DPO ($1.4 \times 10^{-6} \text{ mol dm}^{-3}$) in aqueous solutions containing γ -CD ($3.0 \times 10^{-3} \text{ mol dm}^{-3}$) and various concentrations of PeOH. Concentration of PeOH: (1) 0, (2) 9.20×10^{-4} , (3) 2.76×10^{-3} , (4) 9.20×10^{-3} , and (5) $2.76 \times 10^{-2} \text{ mol dm}^{-3}$. $\lambda_{\text{ex}} = 300 \text{ nm}$.

($1.4 \times 10^{-6} \text{ mol dm}^{-3}$) in γ -CD ($3.0 \times 10^{-3} \text{ mol dm}^{-3}$) solution containing various concentrations of PeOH. When the PeOH concentration is raised, the fluorescence intensity is reduced. This spectral change is similar to that for the increase in the γ -CD concentration in the absence of PeOH (Figure 2). The fluorescence spectral change (Figure 5) as well as the absorption spectral change (Figure 4) indicates the formation of the inclusion complex among γ -CD, PeOH, and 2,4-DPO. To determine the stoichiometry of the ternary γ -CD–PeOH–2,4-DPO inclusion complex, we applied a continuous variation method using the fluorescence intensity, keeping the sum (C_0) of the concentrations of γ -CD and PeOH at $1.0 \times 10^{-2} \text{ mol dm}^{-3}$ (Figure 6). In Figure 6, the open circles show the observed fluorescence intensity of 2,4-DPO. The upper curve (solid curve) exhibits the fluorescence intensity calculated under the assumption that the ternary inclusion complex among γ -CD, PeOH, and 2,4-DPO is not formed (only the 2:1 γ -CD–2,4-DPO inclusion complex is formed). The closed circles show the change in the fluorescence intensity, which is the difference between the calculated fluorescence intensity (the value on the upper curve) and the observed fluorescence intensity (open circle).

Because the absorbance at excitation wavelength is very small in this study, the fluorescence intensity is proportional to the concentration of the fluorescent species. Taking into account the γ -CD cavity size and the dimensions of the alkyl chain of PeOH, it is likely that the γ -CD–PeOH–2,4-DPO inclusion complex contains one or two PeOH molecules, because two γ -CD molecules are included within the 2:1 γ -CD–2,4-DPO inclusion complex. Under the assumption that two PeOH molecules are included in the ternary γ -CD–PeOH–2,4-DPO inclusion complex, therefore, the stoichiometric ratio of the ternary inclusion complex is 2:2:1 for γ -CD, PeOH, and 2,4-DPO. The fluorescence intensity (I_f^{ic}) of the 2:2:1 γ -CD–PeOH–2,4-DPO inclusion complex ($(\gamma\text{-CD})_2 \cdot (\text{PeOH})_2 \cdot 2,4\text{-DPO}$) is proportional to the concentration of the ternary 2:2:1 inclusion complex:

$$\begin{aligned} I_f^{\text{ic}} &= c[(\gamma\text{-CD})_2 \cdot (\text{PeOH})_2 \cdot 2,4\text{-DPO}] \\ &= cK'[\gamma\text{-CD}]^2[\text{PeOH}]^2[2,4\text{-DPO}], \end{aligned} \quad (4)$$

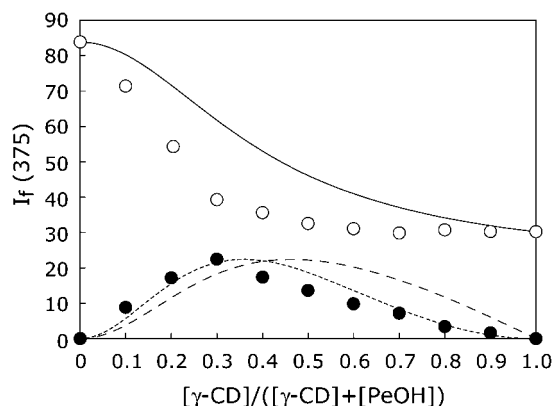


Figure 6. Continuous variation plot for the fluorescence intensity of 2,4-DPO ($1.4 \times 10^{-6} \text{ mol dm}^{-3}$) in aqueous solution containing γ -CD and PeOH. The sum of the concentrations of γ -CD and PeOH has been fixed at $1.0 \times 10^{-2} \text{ mol dm}^{-3}$. The upper curve (solid curve) exhibits fluorescence intensity calculated under the assumption that the γ -CD–PeOH–2,4-DPO inclusion complex is not formed. Open circles exhibit the observed fluorescence intensity. Closed circles exhibit the change in the fluorescence intensity, which is the difference between the calculated fluorescence intensity (the value on the upper curve) and the observed fluorescence intensity (open circle). The dotted and dashed curves are calculated assuming that the 2:2:1 and 2:1:1 γ -CD–PeOH–2,4-DPO inclusion complexes are formed, respectively, and assuming that the initial 2,4-DPO concentration is expressed by the sum of the concentrations of free 2,4-DPO and the 2:1 γ -CD–2,4-DPO inclusion complex. $\lambda_{\text{ex}} = 300 \text{ nm}$. $\lambda_{\text{obs}} = 375 \text{ nm}$.

where c is an instrumental constant and K' is the equilibrium constant for the formation of the ternary inclusion complex. Assuming that the initial concentration ($[2,4\text{-DPO}]_0$) of 2,4-DPO is expressed as the sum of the concentrations of free 2,4-DPO and the 2:1 γ -CD–2,4-DPO inclusion complex, eq 4 is rewritten as

$$I_f^{\text{ic}} = cK'[\gamma\text{-CD}]^2(C_0 - [\gamma\text{-CD}])^2[2,4\text{-DPO}]_0 / (1 + K_1[\gamma\text{-CD}]^2). \quad (5)$$

The calculated curve (dotted curve) for the fluorescence intensity, which is normalized to the maximum value for the closed circles in Figure 6, fits the observed data (closed circles), suggesting that two PeOH molecules are included within the γ -CD–PeOH–2,4-DPO inclusion complex; the 2:2:1 γ -CD–PeOH–2,4-DPO inclusion complex is formed. The calculated curve is maximized at a $[\gamma\text{-CD}]/([\gamma\text{-CD}] + [\text{PeOH}])$ value of 0.36. It should be noted that this value does not show a molar ratio of γ -CD to PeOH in the γ -CD–PeOH–2,4-DPO inclusion complex.

Taking into account the 2,4-DPO concentration in the ternary inclusion complex, the initial concentration of 2,4-DPO is expressed as the sum of the concentrations of free 2,4-DPO, the 2:1 γ -CD–2,4-DPO inclusion complex, and the ternary inclusion complex. In this case, the fluorescence intensity of the ternary inclusion complex is represented by

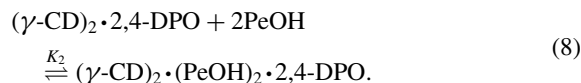
$$I_f^{\text{ic}} = cK'[\gamma\text{-CD}]^2(C_0 - [\gamma\text{-CD}])^2[2,4\text{-DPO}]_0 / (1 + K_1[\gamma\text{-CD}]^2 + K'[\gamma\text{-CD}]^2[\text{PeOH}]^2). \quad (6)$$

If $4.75 \times 10^9 \text{ mol}^{-2} \text{ dm}^6$ is used as the K' value ($K' = K_1K_2$; see below), the curve calculated with eq 6 has a maximum at a $[\gamma\text{-CD}]/([\gamma\text{-CD}] + [\text{PeOH}])$ value of 0.36, which is the same value as that calculated with eq 5, although the curve calculated from eq 6 is slightly broadened in shape compared to the curve calculated from eq 5.

If the ternary inclusion complex contains a single PeOH molecule, the fluorescence intensity of the ternary inclusion complex, under the assumption of $[2,4\text{-DPO}]_0 = [2,4\text{-DPO}] + [(\gamma\text{-CD})_2 \cdot 2,4\text{-DPO}]$, is represented as

$$I_f^{\text{ic}} = c'K''[\gamma\text{-CD}]^2(C_0 - [\gamma\text{-CD}])[2,4\text{-DPO}]_0 / (1 + K_1[\gamma\text{-CD}]^2). \quad (7)$$

Here, c' is an experimental constant, and K'' is the equilibrium constant for the formation of the 2:1:1 $\gamma\text{-CD}$ -PeOH-2,4-DPO inclusion complex. The calculated curve for the fluorescence intensity, which is normalized at the maximum value of the closed circles, is exhibited as a dashed curve in Figure 6. The dashed curve is maximized at a $[\gamma\text{-CD}]/([\gamma\text{-CD}] + [\text{PeOH}])$ value of 0.46. As described above, this value does not show a molar ratio of $\gamma\text{-CD}$ to PeOH in the $\gamma\text{-CD}$ -PeOH-2,4-DPO inclusion complex. The dashed curve does not fit the observed data (closed circles), supporting that the $\gamma\text{-CD}$ -PeOH-2,4-DPO inclusion complex contains two PeOH molecules.



Here, K_2 is the equilibrium constant for the formation of the 2:2:1 $\gamma\text{-CD}$ -PeOH-2,4-DPO inclusion complex. For a 2,4-DPO solution containing $\gamma\text{-CD}$ and PeOH, the fluorescence intensity is represented by

$$I_f = d[2,4\text{-DPO}] + e[(\gamma\text{-CD})_2 \cdot 2,4\text{-DPO}] + f[(\gamma\text{-CD})_2 \cdot (\text{PeOH})_2 \cdot 2,4\text{-DPO}] \\ = (d + eK_1[\gamma\text{-CD}]^2 + fK_1K_2[\gamma\text{-CD}]^2[\text{PeOH}]^2)[2,4\text{-DPO}]_0 / (1 + K_1[\gamma\text{-CD}]^2 + K_1K_2[\gamma\text{-CD}]^2[\text{PeOH}]^2), \quad (9)$$

where d , e , and f are instrumental constants including the fluorescence quantum yields of free 2,4-DPO, the 2:1 $\gamma\text{-CD}$ -2,4-DPO inclusion complex, and the 2:2:1 $\gamma\text{-CD}$ -PeOH-2,4-DPO inclusion complex, respectively. The ratio of e to d , e/d , at an excitation wavelength of 300 nm has been evaluated to be 0.201 from a simulation, in which the fluorescence intensity of a 2,4-DPO solution without PeOH has been plotted against the $\gamma\text{-CD}$ concentration. Figure 7 exhibits the observed fluorescence intensity of 2,4-DPO in $\gamma\text{-CD}$ ($3.0 \times 10^{-3} \text{ mol dm}^{-3}$) solution as a function of PeOH concentration and the least-squares best fit simulation curve. In this simulation, values of d , f , and K_2 are parameters, while the e/d ratio and the K_1 value have already been obtained. The best fit simulation curve fits the observed data, suggesting that the 2:2:1 $\gamma\text{-CD}$ -PeOH-2,4-DPO inclusion complex is produced in 2,4-DPO solution containing $\gamma\text{-CD}$ and PeOH. From the simulation, the K_2 value is estimated to be $7.78 \times 10^4 \text{ mol}^{-2} \text{ dm}^6$.

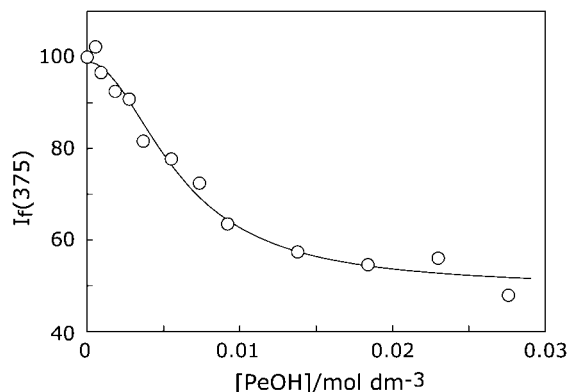


Figure 7. Simulation for the observed fluorescence intensities (open circles) of 2,4-DPO ($1.4 \times 10^{-6} \text{ mol dm}^{-3}$) in aqueous solution containing $\gamma\text{-CD}$ ($3.0 \times 10^{-3} \text{ mol dm}^{-3}$) and PeOH. The best fit simulation curve, which has been based on the scheme involving the formation of the 2:2:1 $\gamma\text{-CD}$ -PeOH-2,4-DPO inclusion complex, has been calculated with the evaluated K_1 value ($61000 \text{ mol}^{-2} \text{ dm}^6$), the evaluated d/c value (0.201), an assumed K_2 value of $7.78 \times 10^4 \text{ mol}^{-2} \text{ dm}^6$, and assumed c and e values of 138 and $49.6 \text{ mol}^{-1} \text{ dm}^3$, respectively. $\lambda_{\text{ex}} = 300 \text{ nm}$. $\lambda_{\text{obs}} = 375 \text{ nm}$.

Table 1. K_2 Values for Various Alcohols

Alcohol	$K_2/\text{mol}^{-2} \text{ dm}^6$
1-Pentanol	7.78×10^4
1-Hexanol	2.58×10^5
1-Heptanol	3.83×10^6
1,9-Nonanediol	7.38×10^5
1,10-Decanediol	4.78×10^7

As in the case of PeOH, similar absorption and fluorescence spectral changes have been observed for 2,4-DPO solution containing $\gamma\text{-CD}$ and 1-hexanol (or 1-heptanol), indicating that the ternary inclusion complex is formed for 1-hexanol (or 1-heptanol). Consequently, the K_2 values for 1-hexanol and 1-heptanol have been evaluated from simulations similar to that for PeOH. These K_2 values are summarized in Table 1. With an increase in the length of the alkyl chain of mono-alcohol, the K_2 value is increased. This finding suggests that the alkyl chain of alcohol is incorporated into the $\gamma\text{-CD}$ cavity. This is reasonable, because the alkyl chain is hydrophobic. Such 2:2:1 inclusion complexes have been reported for the systems of $\beta\text{-CD}$ -alcohol-4*H*-1-benzopyran-4-thione, $\beta\text{-CD}$ -alcohol-azulene, $\beta\text{-CD}$ -alcohol-pyrene, $\gamma\text{-CD}$ -*N,N*-dimethylaniline-perylene, etc.²³⁻²⁶

When diols, 1,9-nonanediol, and 1,10-decanediol, are added to a 2,4-DPO solution containing $\gamma\text{-CD}$ ($3.0 \times 10^{-3} \text{ mol dm}^{-3}$), the 2,4-DPO fluorescence is enhanced. Although, in contrast to mono-alcohol (PeOH etc.), the fluorescence intensity is increased in the presence of the diol, a ternary inclusion complex is most likely formed among $\gamma\text{-CD}$, 2,4-DPO, and the diol. Because, in the ternary inclusion complex, a hydroxy group in diol is in the neighborhood of a 2,4-DPO molecule located within the $\gamma\text{-CD}$ cavities, the hydrophobicity around a 2,4-DPO molecule within the $\gamma\text{-CD}$ cavities seems to be slightly reduced. This may be responsible for the en-

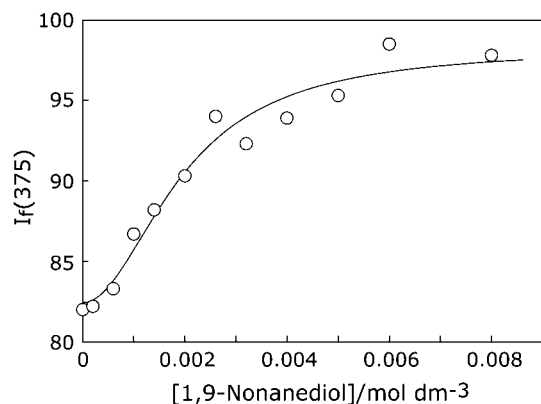


Figure 8. Simulation for the observed fluorescence intensities (open circles) of 2,4-DPO ($1.4 \times 10^{-6} \text{ mol dm}^{-3}$) in aqueous solutions containing γ -CD ($3.0 \times 10^{-3} \text{ mol dm}^{-3}$) and 1,9-nonanediol. The best fit simulation curve, which has been based on the scheme involving the formation of the 2:2:1 γ -CD–1,10-nonanediol–2,4-DPO inclusion complex, has been calculated with the evaluated K_1 value ($61000 \text{ mol}^{-2} \text{ dm}^6$), the evaluated d/c value (0.201), an assumed K_2 value of $7.38 \times 10^5 \text{ mol}^{-2} \text{ dm}^6$, and assumed c and e values of 115 and $98.3 \text{ mol}^{-1} \text{ dm}^3$, respectively. $\lambda_{\text{ex}} = 300 \text{ nm}$. $\lambda_{\text{obs}} = 375 \text{ nm}$.

hancement in the fluorescence intensity of the ternary inclusion complex containing diol. Figure 8 shows the observed fluorescence intensities for 1,9-nonanediol as a function of 1,9-nonanediol concentration. A simulation similar to that for PeOH has been done, and the best fit simulation curve is also shown in Figure 8. From this simulation, the K_2 value for 1,9-nonanediol is estimated to be $7.38 \times 10^5 \text{ mol}^{-2} \text{ dm}^6$ (Table 1). Although the K_2 value for 1,12-dodecanediol could not be evaluated due to the small variation in the fluorescence intensity (the small solubility in water), the K_2 value for 1,10-decanediol has been estimated to be $4.78 \times 10^7 \text{ mol}^{-2} \text{ dm}^6$ (Table 1). The large K_2 value of 1,10-decanediol may imply that a 1,10-decanediol molecule interacts with two γ -CD molecules bound to a 2,4-DPO molecule.

Inclusion of 2,5-DPO by γ -CD. The sample preparation for 2,5-DPO solution by Agbaria and Gill was as follows.^{19,20} (a) Ethanolic solution of 2,5-DPO was allowed to wet the wall of a flask. (b) The solvent was vaporized, leaving the solute on the wall. (c) The γ -CD solution was poured in and incubated for 2 h, so as to allow the sequestering of 2,5-DPO from the wall. In their preparation method, the concentration of 2,5-DPO may be greater than the saturated concentration of 2,5-DPO in water because of the presence of γ -CD.

As in the case of 2,4-DPO, we prepared sample solutions of 2,5-DPO, using aqueous 2,5-DPO solution, in which crystals of 2,5-DPO were submerged in the absence of γ -CD. The 2,5-DPO concentration of the sample solutions prepared according to this method seems to be lower than that used by Agbaria and Gill. The low concentration of 2,5-DPO in this study may induce the inclusion behavior of 2,5-DPO differently from the reported one.

As the γ -CD concentration was increased, the absorption intensity of 2,5-DPO ($7.0 \times 10^{-6} \text{ mol dm}^{-3}$) at the maximum of

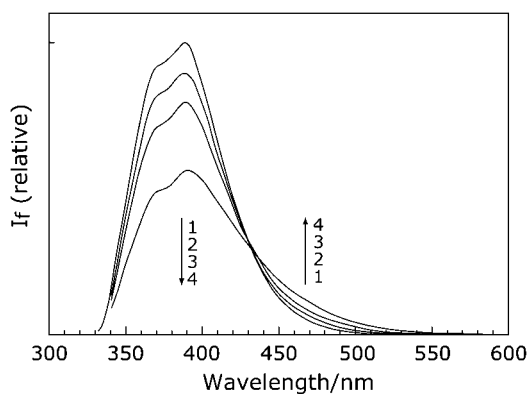


Figure 9. Fluorescence spectra of 2,5-DPO ($7.0 \times 10^{-6} \text{ mol dm}^{-3}$) in aqueous solutions containing various concentrations of γ -CD. Concentration of γ -CD: (1) 0, (2) 1.0×10^{-3} , (3) 3.0×10^{-3} , and (4) $1.0 \times 10^{-2} \text{ mol dm}^{-3}$. $\lambda_{\text{ex}} = 330 \text{ nm}$.

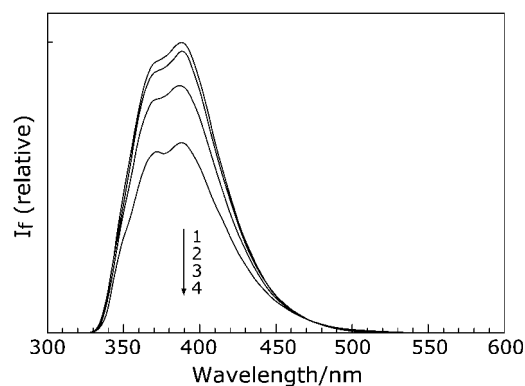


Figure 10. Fluorescence spectra of 2,5-DPO ($7.0 \times 10^{-7} \text{ mol dm}^{-3}$) in aqueous solutions containing various concentrations of γ -CD. Concentration of γ -CD: (1) 0, (2) 1.0×10^{-3} , (3) 3.0×10^{-3} , and (4) $1.0 \times 10^{-2} \text{ mol dm}^{-3}$. $\lambda_{\text{ex}} = 300 \text{ nm}$.

305 nm decreased with an intensity enhancement of the absorption-band tail at longer wavelengths. The absorption spectral change by the addition of γ -CD has suggested the formation of an inclusion complex of γ -CD with 2,5-DPO. When γ -CD is added to 2,5-DPO ($7.0 \times 10^{-6} \text{ mol dm}^{-3}$) solution, the 2,5-DPO fluorescence at 390 nm is reduced in intensity, accompanied by an appearance of a new, broad band at longer wavelengths (Figure 9). The new band can be assigned to the excimer fluorescence of 2,5-DPO.^{19,20} The excimer fluorescence is due to an inclusion complex between γ -CD and 2,5-DPO. As the γ -CD concentration is increased in dilute ($7.0 \times 10^{-7} \text{ mol dm}^{-3}$) solution of 2,5-DPO, on the other hand, the 2,5-DPO fluorescence is decreased in intensity without an appearance of the longer wavelength band (Figure 10). This finding indicates that the species responsible for the excimer fluorescence is not formed at a low concentration of 2,5-DPO. Figure 11 depicts a double-reciprocal plot for the fluorescence intensities of dilute 2,5-DPO solutions containing γ -CD. The plot for the dilute 2,5-DPO solutions exhibits a straight line, indicating that a 1:1 γ -CD–2,5-DPO inclusion complex is formed at low 2,5-DPO concentrations:

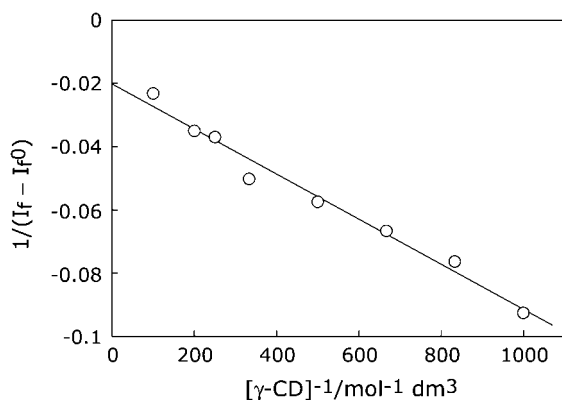
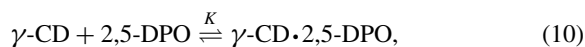


Figure 11. Plot of $1/(I_f - I_f^0)$ against $1/[\gamma\text{-CD}]$ for 2,5-DPO ($7.0 \times 10^{-7} \text{ mol dm}^{-3}$) in aqueous solution containing $\gamma\text{-CD}$. $\lambda_{\text{ex}} = 300 \text{ nm}$. $\lambda_{\text{obs}} = 375 \text{ nm}$.



where $\gamma\text{-CD} \cdot 2,5\text{-DPO}$ is the 1:1 $\gamma\text{-CD}$ –2,5-DPO inclusion complex. A K value of $280 \pm 30 \text{ mol}^{-1} \text{ dm}^3$ is evaluated from the plot shown in Figure 11.

At a low DPO concentration, the stoichiometry of the $\gamma\text{-CD}$ –DPO inclusion complex is 1:1 for 2,5-DPO, whereas it is 2:1 for 2,4-DPO. The fact that the solubility of 2,5-DPO is greater than that of 2,4-DPO seems to influence the inclusion modes of DPOs; because of the high solubility of 2,5-DPO, the hydrophobicity of 2,5-DPO seems to be less than that of 2,4-DPO. This might lead to the formation of the $\gamma\text{-CD}$ –DPO inclusion complexes of different stoichiometry for 2,4- and 2,5-DPO.

As the species responsible for the excimer fluorescence, a 1:2 $\gamma\text{-CD}$ –2,5-DPO inclusion complex (and its aggregate) has been suggested.^{19,20}



where K_3 is the equilibrium constant for the formation of the 1:2 $\gamma\text{-CD}$ –2,5-DPO inclusion complex ($\gamma\text{-CD} \cdot (2,5\text{-DPO})_2$). Because the absorbance of 2,5-DPO at an excitation wavelength is small, the fluorescence intensity is approximately proportional to the concentration of a fluorescent species of 2,5-DPO. In this scheme, therefore, the excimer fluorescence intensity, $I_f(\text{excimer})$, is represented by

$$\begin{aligned} I_f(\text{excimer}) &= g[\gamma\text{-CD} \cdot (2,5\text{-DPO})_2] \\ &= gK_3[\gamma\text{-CD}][2,5\text{-DPO}]^2, \end{aligned} \quad (12)$$

where g is an instrumental constant including the excimer fluorescence quantum yield of the 1:2 $\gamma\text{-CD}$ –2,5-DPO inclusion complex. Besides the equilibrium represented by eq 11, there is an additional equilibrium (eq 10), which describes the formation of the 1:1 $\gamma\text{-CD}$ –2,5-DPO inclusion complex, in 2,5-DPO solution containing $\gamma\text{-CD}$. Consequently, the concentration of free 2,5-DPO is obtained by solving the quadratic equation:

$$2K_3[\gamma\text{-CD}][2,5\text{-DPO}]^2 + (1 + K[\gamma\text{-CD}])[2,5\text{-DPO}] - [2,5\text{-DPO}]_0 = 0. \quad (13)$$

Because the K value for 2,5-DPO has already been evaluated,

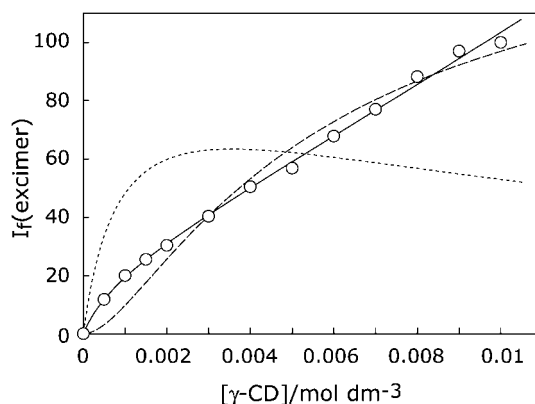


Figure 12. Simulation for the observed excimer fluorescence intensity of 2,5-DPO ($7.0 \times 10^{-6} \text{ mol dm}^{-3}$) in aqueous solution containing $\gamma\text{-CD}$. (a) The best fit simulation curve (dotted curve) has been calculated on the basis of the scheme involving the formation of the 1:1 and 1:2 $\gamma\text{-CD}$ –2,5-DPO inclusion complexes, using the evaluated K_1 value ($280 \text{ mol}^{-1} \text{ dm}^3$), an assumed K_3 value of $2.29 \times 10^7 \text{ mol}^{-2} \text{ dm}^6$, and an assumed g value of $9.60 \times 10^7 \text{ mol}^{-1} \text{ dm}^3$. (b) The best fit simulation curve (dashed curve) has been calculated on the basis of the scheme involving the formation of the 1:1 and 2:2 $\gamma\text{-CD}$ –2,5-DPO inclusion complexes, using the evaluated K_1 value ($280 \text{ mol}^{-1} \text{ dm}^3$), an assumed K_4 value of $1.04 \times 10^4 \text{ mol}^{-1} \text{ dm}^3$, and an assumed h value of $4.04 \times 10^8 \text{ mol}^{-1} \text{ dm}^3$. (c) The best fit simulation curve (solid curve) has been calculated on the basis of the scheme involving the formation of the 1:1, 1:2, and 2:2 $\gamma\text{-CD}$ –2,5-DPO inclusion complexes, using the evaluated K_1 value ($280 \text{ mol}^{-1} \text{ dm}^3$), assumed K_3 and K_4 values of $3.34 \times 10^6 \text{ mol}^{-2} \text{ dm}^6$ and $1.48 \times 10^3 \text{ mol}^{-1} \text{ dm}^3$, and assumed i and j values of 1.69×10^{10} and $2.39 \times 10^6 \text{ mol}^{-1} \text{ dm}^3$, respectively. $\lambda_{\text{ex}} = 330 \text{ nm}$. $\lambda_{\text{obs}} = 500 \text{ nm}$.

the free 2,5-DPO concentration can be calculated assuming a K_3 value. The best fit simulation curve (dotted curve) for the excimer fluorescence intensity, which is based on the scheme involving the formation of the 1:2 $\gamma\text{-CD}$ –2,5-DPO inclusion complex, is shown in Figure 12. This simulation curve does not fit the observed excimer fluorescence data, indicating that the excimer fluorescence is not due to the 1:2 $\gamma\text{-CD}$ –2,5-DPO inclusion complex.

If the 1:2 $\gamma\text{-CD}$ –2,5-DPO inclusion complexes aggregate to produce a 2:4 $\gamma\text{-CD}$ –2,5-DPO inclusion complex, both the 1:2 and 2:4 $\gamma\text{-CD}$ –2,5-DPO inclusion complexes would be responsible for the excimer fluorescence. On the basis of this scheme, we calculated the best fit simulation curve for the excimer fluorescence intensity. However, the best fit simulation curve was similar in shape to that calculated for the scheme involving only the 1:2 $\gamma\text{-CD}$ –2,5-DPO inclusion complex as the species emitting the excimer fluorescence; the best fit simulation curve based on the aggregation of the 1:2 $\gamma\text{-CD}$ –2,5-DPO inclusion complex could not reproduce the observed data.

In several systems, 2:2 CD–guest inclusion complexes are responsible for excimer fluorescence in aqueous solution; the $\beta\text{-CD}$ –naphthalene system, the $\gamma\text{-CD}$ –pyrene system, etc.^{7–10,13} When the 1:1 $\gamma\text{-CD}$ –2,5-DPO inclusion complexes associate to form the 2:2 $\gamma\text{-CD}$ –2,5-DPO inclusion complex,

the excimer fluorescence is most likely due to the 2:2 inclusion complex $(\gamma\text{-CD})_2 \cdot (2,5\text{-DPO})_2$:



where K_4 is the equilibrium constant for the formation of the 2:2 $\gamma\text{-CD}$ –2,5-DPO inclusion complex. In this scheme, the excimer fluorescence intensity is represented by

$$\begin{aligned} I_f(\text{excimer}) &= h[(\gamma\text{-CD})_2 \cdot (2,5\text{-DPO})_2] \\ &= hK^2K_4[\gamma\text{-CD}]^2[2,5\text{-DPO}]^2, \end{aligned} \quad (15)$$

where h is an instrumental constant including the excimer fluorescence quantum yield of the 2:2 $\gamma\text{-CD}$ –2,5-DPO inclusion complex. The concentration of free 2,5-DPO can be obtained by solving the quadratic equation:

$$2K^2K_4[\gamma\text{-CD}]^2[2,5\text{-DPO}]^2 + (1 + K[\gamma\text{-CD}])[2,5\text{-DPO}] - [2,5\text{-DPO}]_0 = 0. \quad (16)$$

The best fit simulation curve (dashed curve), which has been calculated assuming a K_4 value, is also exhibited in Figure 12. As in the case of the first scheme in which the 1:2 $\gamma\text{-CD}$ –2,5-DPO inclusion complex is responsible for the excimer fluorescence, the best fit simulation curve based on the formation of the 2:2 inclusion complex does not reproduce the observed excimer fluorescence intensities.

Thus, we have tried to simulate on the basis of a scheme, in which both the 1:2 and 2:2 $\gamma\text{-CD}$ –2,5-DPO inclusion complexes are responsible for the excimer fluorescence. In this case, the excimer fluorescence intensity is given by

$$\begin{aligned} I_f(\text{excimer}) &= i[\gamma\text{-CD} \cdot (2,5\text{-DPO})_2] \\ &\quad + j[(\gamma\text{-CD})_2 \cdot (2,5\text{-DPO})_2] \\ &= (iK_3 + jK^2K_4[\gamma\text{-CD}][\gamma\text{-CD}][2,5\text{-DPO}]^2, \end{aligned} \quad (17)$$

where i and j are instrumental constants including the excimer fluorescence quantum yields of the 1:2 and 2:2 $\gamma\text{-CD}$ –2,5-DPO inclusion complexes, respectively. The concentration of free 2,5-DPO can be calculated by solving the quadratic equation:

$$2(K^2K_4[\gamma\text{-CD}] + K_3)[\gamma\text{-CD}][2,5\text{-DPO}]^2 + (1 + K[\gamma\text{-CD}])[2,5\text{-DPO}] - [2,5\text{-DPO}]_0 = 0. \quad (18)$$

Figure 12 shows the best fit simulation curve (solid curve), for which values of K_3 and K_4 are assumed to be $3.34 \times 10^6 \text{ mol}^{-2} \text{ dm}^6$ and $1.48 \times 10^3 \text{ mol}^{-1} \text{ dm}^3$, respectively. This simulation curve well fits the observed fluorescence intensity data, indicating that the excimer fluorescence is due to both the 1:2 and 2:2 $\gamma\text{-CD}$ –2,5-DPO inclusion complexes.

Our conclusion that the excimer fluorescence is due to both the 1:2 and 2:2 $\gamma\text{-CD}$ –2,5-DPO inclusion complexes is different from the conclusion of Agbaria and Gill, who have assigned the 1:2 $\gamma\text{-CD}$ –2,5-DPO inclusion complex (and its aggregate) as the species emitting the excimer fluorescence.^{19,20} However, the 2,5-DPO concentration, which they used, is probably higher than that in this study. At higher concentrations of 2,5-DPO, the concentration of the 2:2 $\gamma\text{-CD}$ –2,5-DPO inclusion complex may be negligible relative to that of the 1:2 $\gamma\text{-CD}$ –2,5-DPO inclusion complex. In addition, there may be the possibility that the 1:2 inclusion complexes

aggregate at higher concentrations of 2,5-DPO. Consequently, our conclusion concerning the species responsible for the excimer fluorescence does not seem to be inconsistent with the conclusion of Agbaria and Gill.

Conclusion

In aqueous solution, $\gamma\text{-CD}$ forms a 2:1 inclusion complex with 2,4-DPO, whereas $\beta\text{-CD}$ forms a 1:1 inclusion complex with 2,4-DPO. Addition of alcohol to a 2,4-DPO solution containing $\gamma\text{-CD}$ results in the formation of a 2:2:1 $\gamma\text{-CD}$ –alcohol–2,4-DPO inclusion complex. The equilibrium constant for the formation of the ternary inclusion complex increases with increasing length of the alkyl chain of alcohol (from 1-pentanol to 1-heptanol). The same is true for diols (1,9-nonanediol and 1,10-decanediol). At a low 2,5-DPO concentration such as $7.0 \times 10^{-7} \text{ mol dm}^{-3}$, $\gamma\text{-CD}$ forms a 1:1 inclusion complex with 2,5-DPO. At a high 2,5-DPO concentration such as $7.0 \times 10^{-6} \text{ mol dm}^{-3}$, on the other hand, excimer fluorescence is observed in the presence of $\gamma\text{-CD}$. The excimer fluorescence is due to the 2:1 $\gamma\text{-CD}$ –2,5-DPO inclusion complex and the 2:2 $\gamma\text{-CD}$ –2,5-DPO inclusion complex.

References

- 1 W. Saenger, *Angew. Chem., Int. Ed. Engl.* **1980**, *19*, 344.
- 2 R. J. Clarke, J. H. Coates, S. F. Lincoln, *Carbohydr. Res.* **1984**, *127*, 181.
- 3 H. Hirai, N. Toshima, S. Uenoyama, *Bull. Chem. Soc. Jpn.* **1985**, *58*, 1156.
- 4 R. L. Schiller, S. F. Lincoln, J. H. Coates, *J. Chem. Soc., Faraday Trans. 1* **1986**, *82*, 2123.
- 5 S. Hamai, *Bull. Chem. Soc. Jpn.* **2000**, *73*, 861.
- 6 P. R. Sainz-Rozas, J. R. Isasi, G. Gonzalez-Gaitano, *J. Photochem. Photobiol., A* **2005**, *173*, 319.
- 7 N. Kobayashi, R. Saito, H. Hino, Y. Hino, A. Ueno, T. Osa, *J. Chem. Soc., Perkin Trans. 2* **1983**, 1031.
- 8 W. G. Herkstroeter, P. A. Martic, S. Farid, *J. Chem. Soc., Perkin Trans. 2* **1984**, 1453.
- 9 W. G. Herkstroeter, P. A. Martic, T. R. Evance, S. Farid, *J. Am. Chem. Soc.* **1986**, *108*, 3275.
- 10 S. Hamai, *J. Phys. Chem.* **1989**, *93*, 6527.
- 11 S. Tamagaki, K. Fukuda, H. Maeda, N. Mimura, W. Tagaki, *J. Chem. Soc., Perkin Trans. 2* **1995**, 389.
- 12 S. Hamai, *Bull. Chem. Soc. Jpn.* **1996**, *69*, 543.
- 13 S. Hamai, *Bull. Chem. Soc. Jpn.* **1982**, *55*, 2721.
- 14 T. Tamaki, T. Kokubu, T. Ichimura, *Tetrahedron* **1987**, *43*, 1485.
- 15 T. C. Barros, K. Stefaniak, J. F. Holzwarth, C. Bohne, *J. Phys. Chem. A* **1998**, *102*, 5639.
- 16 K. Uekama, M. Otagiri, Y. Kanie, S. Tanaka, K. Ikeda, *Chem. Pharm. Bull.* **1975**, *23*, 1421.
- 17 M. V. Rekharsky, M. P. Mayhew, R. N. Goldberg, P. D. Ross, Y. Yamashoji, Y. Inoue, *J. Phys. Chem. B* **1997**, *101*, 87.
- 18 S. Hamai, *Bull. Chem. Soc. Jpn.* **2006**, *79*, 1039.
- 19 R. A. Agbaria, D. Gill, *J. Photochem. Photobiol., A* **1994**, *78*, 161.
- 20 R. A. Agbaria, D. Gill, *J. Phys. Chem.* **1988**, *92*, 1052.
- 21 A. Harada, M. Okada, J. Li, M. Kamachi, *Macromolecules* **1995**, *28*, 8406.
- 22 M. Kodaka, *J. Am. Chem. Soc.* **1993**, *115*, 3702.
- 23 M. Milewski, W. Augustyniak, A. Maciejewski, *J. Phys.*

Chem. A **1998**, 102, 7427.

24 S. Hamai, T. Ikeda, A. Nakamura, H. Ikeda, A. Ueno, F. Toda, *J. Am. Chem. Soc.* **1992**, 114, 6012.

25 A. Munoz de la Pena, T. T. Ndou, J. B. Zung, K. L.

Greene, D. H. Live, I. M. Warner, *J. Am. Chem. Soc.* **1991**, 113, 1572.

26 S. Hamai, *Bull. Chem. Soc. Jpn.* **1991**, 64, 431.